Deep–Sea Research I 170 (2021) 103494

Contents lists available at ScienceDirect

Deep-Sea Research Part I

journal homepage: http://www.elsevier.com/locate/dsri

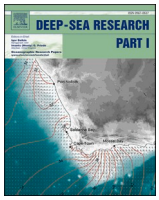

Come rain or shine: Depth not season shapes the active protistan community at station ALOHA in the North Pacific Subtropical Gyre

Gerid A. Ollison [a,*], Sarah K. Hu [b], Lisa Y. Mesrop [c], Edward F. DeLong [d], David A. Caron [a]

[a] Department of Biological Sciences, University of Southern California, 3616 Trousdale Parkway, Los Angeles, CA. 90089-0371, USA
[b] Woods Hole Oceanographic Institution, Marine Chemistry and Geochemistry, 266 Woods Hole Rd., Woods Hole, MA, 02543, USA
[c] Department of Ecology, Evolution and Marine Biology, University of California Santa Barbara, Santa Barbara, CA, 93106, USA
[d] Daniel K. Inouye Center for Microbial Oceanography, Research and Education, University of Hawai'i, Manoa, Honolulu, HI, 96822, USA

ARTICLE INFO

Keywords:
Protistan diversity
Microbial ecology
Hawaii ocean time series
North pacific subtropical gyre

ABSTRACT

Protists are extremely diverse morphologically and physiologically, and they play important ecological roles at multiple trophic levels as primary producers and consumers in nearly all microbial communities. In spite of their fundamental importance in marine ecosystems, protistan diversity and distribution has yet to be comprehensively characterized in much of the world ocean, particularly in the vast expanses below the euphotic zone. We examined protistan community structure and species diversity in the oligotrophic North Pacific Subtropical Gyre. Our primary goal was to better characterize the breadth of metabolically active protistan species throughout the water column spanning 12 depths from 5 m to 770 m (~600 m below the euphotic zone) across three seasons using 18S rRNA gene V4 amplicon sequencing of RNA (cDNA).

Protistan community structure changed markedly across relatively narrow ranges of increasing depths between 75 m-100 m, and again between 175 m-300 m. Changes were driven by depth-specific distributions among major protistan taxa associated with the upper mixed layer, deep chlorophyll maximum and aphotic zone, respectively, in this permanently stratified water column. Diatoms and some heterotrophic protists (MAST, choanoflagellates) were important contributors in the upper mixed layer, while haptophytes and pelagophytes increased in relative abundances in the lower euphotic zone. Radiolaria, ciliates and syndinians (putative parasitic protists within the order Syndiniales) increased in relative abundances below the euphotic zone. Overall, the highest taxonomic richness of amplicon sequence variants (ASVs) was observed in aphotic samples. Additionally, the dominant ASVs within some taxonomic groups that were observed in deep water were different than those observed in the upper water column, implying adaptations to specific depth strata rather than passive transport of surface-dwelling species. In contrast to depth-related changes, seasonal changes in protistan community structure were not significant.

1. Introduction

Unicellular eukaryotes (protists) are fundamental components of nearly every microbial assemblage. The immense ranges of sizes, forms, and trophic lifestyles of protists enable them to influence energy and carbon flow across marine food webs through primary production, phagotrophic consumption, and parasitic associations (Caron et al., 2012; Worden et al., 2015). Protistan primary producers are ubiquitous in the euphotic zone of the global ocean (de Vargas et al., 2015), and account for nearly half of the annual pelagic production (Field et al., 1998). Episodic algal blooms can also be a significant source of carbon flux to the deep ocean (Scharek et al., 1999).

Processes that remineralize organic carbon or transfer it to higher trophic levels in surface waters, or export it out of the photic zone, are directly mediated by diverse assemblages of heterotrophic protists (Caron, 1994; Sherr and Sherr, 2002; Calbet and Saiz, 2005) including phagotrophic, mixotrophic, and parasitic species. These species have a profound impact on carbon cycling and ecosystem function through positive and negative trophic interactions (Lafferty et al., 2006; Poulin, 2010) and by acting as a significant source of bacterial mortality (Hartmann et al., 2012; Unrein et al., 2014; Brum et al., 2014). Although we are gaining a clearer picture of the diversity and distribution of protists thanks to recent advances in high-throughput sequencing technology, reference databases, and global oceanographic surveys

* Corresponding author.
E-mail address: gollison@usc.edu (G.A. Ollison).

https://doi.org/10.1016/j.dsr.2021.103494
Received 10 August 2020; Received in revised form 10 January 2021; Accepted 8 February 2021
Available online 12 February 2021

(Guillou et al., 2008, 2013; Lima-Mendez et al., 2015), species richness is not fully characterized in most free-living communities, especially below the euphotic zone in the open ocean. Understanding these aspects of community ecology are essential for modeling ecosystem function and response to environmental change (Ward et al., 2012; Worden et al., 2015; Ward and Follows, 2016).

Protistan species richness and diversity have traditionally been documented using microscopy, and the primary taxonomy of these species is still based on morphological descriptions. However, genetic studies of diversity that have become commonplace over the past two decades have altered our comprehension of the species richness and community structure of free-living protistan communities (Stoeck et al., 2009; Edgcomb and Pachiadaki, 2014; de Vargas et al., 2015; Hu et al., 2016b; Giner et al., 2020). Considerable effort is now being expended on merging genetic, morphological and physiological information into a single species concept (Berney et al., 2017). Such a merged species concept will greatly facilitate the interpretation of environmental surveys of protistan genetic diversity in an ecological context.

Most studies of marine protistan diversity have been conducted at specific geographical locations and/or with limited temporal coverage, although a few studies have been carried out across large expanses of the global ocean, or have examined seasonality. The latter studies have begun to establish the broader spatiotemporal distributions of protists (de Vargas et al., 2015; Lima-Mendez et al., 2015; Pernice et al., 2015; Hu et al., 2016a; Giner et al., 2019). However, relatively few studies dedicated to the study of protistan assemblages of the deep ocean have been conducted (Countway et al., 2007; Edgcomb et al., 2011; Orsi et al., 2011; Pernice et al., 2016; Giner et al., 2016, 2020; Xu et al., 2017; Obiol et al., 2020; Canals et al., 2020; Mars Brisbin et al., 2020), some of which have been targeted at specific benthic features such as hydrothermal vents (Coyne et al., 2013; Edgcomb, 2016; Pasulka et al., 2019).

The North Pacific Subtropical gyre (NPSG) is the largest contiguous biome on the planet and accounts for a significant amount of organic carbon production and biogeochemical cycling. The biological, chemical and physical aspects of the NPSG have been studied regularly and continuously since 1988 at station ALOHA through the Hawai'i Ocean Time-series program (HOT) (Karl and Church, 2014). A broad range of habitats characterize station ALOHA extending from the persistently warm, nutrient-starved, light-saturated upper mixed layer to the cold, nutrient-rich, light-limited regions of the lower euphotic and below. We have gained a lot of insight about bacterial diversity and vertical stratification in this oligotrophic regime via high-throughput sequencing (HTS) analyses (metagenomic, metatranscriptomic, and metabarcode) (Konstantinidis et al., 2009; Malmstrom et al., 2010; Mende et al., 2017; Boeuf et al., 2019), and other molecular and phylogenetic-based methodologies (Karner et al., 2001; Karl and Church, 2014), however the extent of protistan species richness and vertical distribution below the euphotic zone at station ALOHA has not been comprehensively characterized (Pasulka et al., 2013; Rii et al., 2016b).

We employed 18S rRNA gene V4 amplicon sequencing of RNA (cDNA) to characterize the breadth of metabolically active protistan taxa and their vertical distribution from 12 depths spanning 5 m–770 m across three seasons at station ALOHA. The protistan community changed markedly across two narrow ranges of increasing depth (between 75 m-100 m and 175 m–300 m), forming three community zones encompassing the upper euphotic (5 m–75 m), lower euphotic (100 m–175 m), and aphotic depths (300 m–770 m). Differences between the communities were a consequence of distinct distributional patterns of major protistan groups. A photosynthetic community composed of dinoflagellates, stramenopiles and haptophytes collectively occupied the euphotic zone, however, relative abundances of these groups differed between the light-saturated upper mixed layers (≤75 m) and the deep chlorophyll maximum (DCM; 100 m–150m). Heterotrophic protists, primarily alveolates and rhizarians, colonized the entire water column but increased in relative abundances and changed in taxonomic composition with depth. The exceptions, small heterotrophic flagellates (MArine STramenopiles and choanoflagellates), were more common at shallower depths. Parasites colonized the entire water column, increased markedly with depth, and exhibited species-specific vertical distributions. Collectively, aphotic depths exhibited the highest diversity and greater numbers of unclassifiable ASVs (although unclassifiable ASVs were a small component of total sequence counts). Compared to depth-dependent shifts in community composition, changes associated with season were insignificant at the study site with few exceptions.

2. Materials and methods

Sequencing of environmental 18S rRNA gene transcripts (RNA) were carried out on samples collected at 12 depths from 5 m to 770 m in the North Pacific Subtropical Gyre (NPSG) to assess protistan species richness and diversity across seasons and depths spanning the euphotic and aphotic zones. Sampling was conducted on four dates spanning a one-year period.

2.1. Sample collection

Samples were collected during four expeditions at station ALOHA (22.75°N, 158°W) as part of the Hawai'i Ocean Time-series (HOT) program from December 2014 to December 2015 (HOT 268–121,614, HOT 271–042,415, HOT 275–081,115, HOT 279–120,815) (Karl and Church, 2014). Water was collected from twelve depths spanning euphotic and aphotic depths: 5 m, 25 m, 45 m, 75 m, 100 m, 125 m, 150 m, 175 m, 300 m, 400 m, 500 m, 770 m. No sample was taken at 45 m in April 2015. Each of the 12 depths were collected using a 24-place rosette equipped with 12-L Niskin bottles. Real-time nitrate, temperature, salinity, dissolved oxygen, and chlorophyll *a* concentrations were collected with a vertically mounted SBE-9/11 plus CTD equipped with dual C, T, DO sensors. All CTD data are available at hahana. soest. hawaii.edu/hot/hot-dogs/interface.html.

Seawater was prefiltered through an 80 μm Nitex mesh to minimize the contribution of metazoa, and 3.5 L aliquots of each sample were filtered (≤15 psi) onto 25 mm 0.2 μm Supor PES Membrane Disc filters (Pall, USA). Samples were stored in 300 μl of RNALater (Sigma-Aldrich, #R0901) and frozen at -80 C for later RNA extraction.

2.2. Nucleic acid extraction and sequencing

Samples were thawed on ice, centrifuged for 1 min at 10,000 rpm, and RNALater was removed before subsequent extraction steps. Total RNA was extracted using the All Prep DNA/RNA Mini kit (Qiagen, Valencia, CA #80204). Genomic DNA was removed during RNA extraction using an RNase-Free DNase (Qiagen, #79254). DNA removal was confirmed by lack of amplification of extracted DNA in downstream PCR reactions. RNA was reverse transcribed to cDNA using the iScript Reverse Transcription Supermix with random hexamers (Bio-Rad Laboratories, Hercules #170–8840).

Samples were PCR amplified with Q5 High-Fidelity 2x Master Mix (NEB, #M0492S) 18S 565 F (5′-CCAGCASCYGCGGTAATTCC-3′) and 948 R (5′-ACTTTCGTTCTTGATYRA-3′) primers (Stoeck et al., 2010). PCR reactions were carried out in two steps due to the differences in annealing temperature between the primer pair. Reactions consisted of a 98 °C denaturation step for 2 min, followed by 10 cycles of 98 °C for 10s, 53 °C for 30s and 72 °C for 30s. Next, 15 cycles of 98 °C for 10s, 48 °C for 30s and 72 °C for 30s, followed by a final elongation step at 72 °C for 2min. PCR products were purified using Agencourt AMPure XP beads per our established lab protocol (dx.doi.org/10.17504/protocols.io.hdmb246), and indexed using Illumina-specific P5 and P7 indices. Samples were quantified using a Qubit 2.0 fluorometer (ThermoFisher Scientific, #Q32866), quality checked on an Agilent Bioanalyzer 2100 (Agilent Technologies, Santa Clara), and normalized prior to sequencing (dx.doi.org/10.17504/protocols.io.rfvd3n6). Paired-end sequencing (250 × 250 bp) was performed via Illumina MiSeq (Laragen Inc. Culver

City, CA).

2.3. Sequence analysis

Amplicon Sequence Variants (ASVs) (Callahan et al., 2017) were generated using DADA2 (Callahan et al., 2016) via Qiime2 v2018.11 (Bolyen et al., 2019) from sequenced 18S rRNA gene transcripts (RNA) to investigate the metabolically active taxa within the protistan community (Blazewicz et al., 2013). Briefly, reads from each sample were demultiplexed with the Qiime2 demux function. Barcodes, primers, and low-quality bases at the ends of both forward and reverse reads were removed using the trim and trunc options of the Qiime2 DADA 2 plugin. Sequences were quality filtered, denoised, merged, dereplicated, chimera checked, and split into amplicon sequence variants (ASV) using the Qiime2 DADA 2 plugin default parameters. Taxonomic classifications were assigned at 90% confidence using the Qiime2 pre-fitted sklearn-based taxonomy classification and the latest iteration of the PR2 database (Guillou et al., 2013) (v.12.1; https://github.com/pr2database/pr2database). Taxonomic classification was attempted using the SILVA 18S rRNA gene database (v.132) (Pruesse et al., 2007) for ASVs lacking taxonomic identification via the PR2 database. Individual abundant representative ASVs of interest lacking taxonomic information within either database were further investigated using NCBI BLAST.

Further quality assessment and final sequence analysis was conducted in R (R_Core_Team, 2020) v3.5.1 "Feather Spray." ASVs that contained one sequence within the entire dataset were removed, and raw ASV sequence counts were subsequently normalized using the Trimmed Mean of M-values transformation (TMM) prior to all downstream analysis using edgeR v.3.30. TMM normalization was chosen because it allowed the retention of all sequenced reads, and has been shown to be a robust method of normalization when employed with Bray-Curtis dissimilarities (Weiss et al., 2017). Taxonomic group names were manually curated at approximately phylum level for easier ecological interpretation (Fig. 1), and manually assigned at higher levels of resolution when necessary (Figures S2, S3).

Alpha diversity statistics (Shannon and inverse Simpson) were calculated in R using the diversity function (Vegan v2.4–2). Total species richness was estimated by totaling the number of unique ASVs. Non-metric multidimensional scaling of Bray-Curtis dissimilarities was calculated in R using the metaMDS function (Vegan v2.4–2). UpSet plots were generated from a binary ASV table (constructed from the TMM normalized ASV table) where an ASV with greater or less than 10 reads in a sample was given a 1 for presence or 0 for absence, respectively. The UpSet R package was used to generate upset plots (Conway et al., 2017). Cluster dendrograms were generated by combining pairwise Euclidean distances with the average method of clustering. Briefly, after quantifying distances between samples (Euclidean), pairwise averages were used as the distances between other pairs and clusters.

2.4. Data accessibility

Raw sequence data are available on NCBI under accession number SRP110191. The quality-filtered ASV table used in this study is available as a comma-separated table (Table S1). All R scripts for plots, data quality filtering and analysis can be found at https://github.com/theOlligist/ALOHA-SpatioTemporal.

3. Results

3.1. Environmental conditions at the study site

Physical and chemical properties of the water column at station ALOHA were generally consistent with long-term measurements conducted as part of the HOT program. Surface temperatures varied by less than 4 °C across the three sampled seasons, which basically encompassed the full seasonal range generally observed at station ALOHA (Figure S1A). The depth of the seasonal thermocline was approximately 45 m in August, deepening to approximately 120 m in December

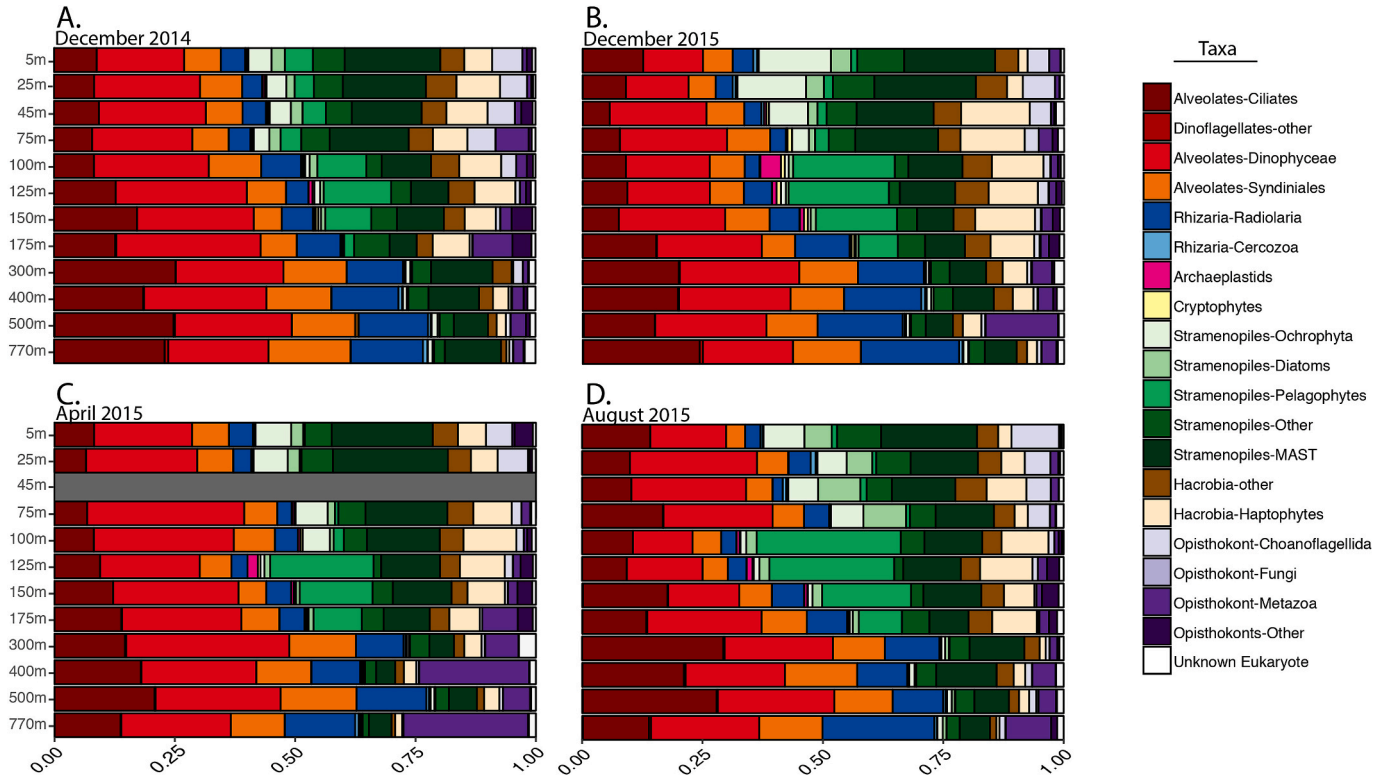

Fig. 1. Relative abundance of rRNA-based ASVs across all depths (5 m–770 m) from three seasons at station ALOHA; December (A–B), April (C), and August (D) are shown. Colors represent major protistan taxonomic groups. No samples were taken at 45 m during the month of April 2015.

(Figure S1A; http://hahana.soest.hawaii.edu/hot/hot-dogs/interface.html). August and December were the only months with significant seasonal variation in temperature and chlorophyll *a* values. Nitrate values in the upper euphotic were between 1-5 μM/L throughout the year with the highest recorded values in the December months and the shallowest nitricline (~120 m) in the month of August (Figure S1B). Oxygen depth profiles were not noticeably variable across seasons, with the exception of a spike at 65 m in August. Oxygen values ranged from 180 to 210 μM/kg from the surface to the oxycline. The latter feature began at approximately 300 m, with oxygen values decreasing to <50 μM/kg by 600 m (Figure S1C). Chlorophyll *a* concentrations at the DCM were seasonally variable with the highest concentrations observed in August (0.75 μg/L) (Figure S1D).

3.2. Protistan community richness and diversity varied across depths and seasons

The primary aim of this study was to characterize protistan diversity within the sunlit and aphotic zones at station ALOHA, and compare the influences of depth and seasonal changes. A total of 2.6 million rRNA transcript reads were obtained from 47 samples after quality filtering and the removing chimeric sequences (Table S2). The quality filtered reads resulted in a total of 11,538 Amplicon Sequence Variants (ASVs) representing species-level to strain-level distinctions for most protistan taxa (Caron and Hu, 2018; Table S2). Overviews of community composition are given here, while more detailed descriptions are provided in the Supplemental Materials.

Stramenopila, Alveolata, and Rhizaria (SAR) taxa constituted more than 50% of the community throughout the entire water column during every season (Fig. 1; Supplemental Materials). MAST was the only classifiable stramenopile group that averaged more than a few percent of the community at all depths and across all seasons (12%), with MAST-3 dominant among these taxa. Three other relatively abundant stramenopile groups were observed in the study primarily above 175 m. Photosynthetic stramenopiles were composed of diatoms, pelagophytes, and 'other ochrophytes', and were most abundant during August (Fig. 1, S2B; Table S1). The diatom assemblage was composed of 16 classifiable taxa (out of 322 ASVs; Figure S2B), the majority of which exhibited maximal abundances between 5 m and 75 m, and were 4-fold more abundant in August than any other month sampled. Unclassifiable ochrophyte ASVs mirrored diatom spatiotemporal distributions, implying that they may be diatoms that were not taxonomically resolved (Fig. 1). In contrast, pelagophytes exhibited higher relative abundances at the DCM and near the base of the euphotic zone (100 m–150 m; Fig. 1).

Ciliates, dinoflagellates, and syndinians were commonly observed alveolates in this study (Fig. 1; Supplemental Materials). Dinoflagellates were the most abundant major taxonomic group within the protistan community, accounting for >20% of the community at every depth and during every month. There were 24 classifiable dinoflagellate taxa (out of 1449 ASVs) distributed throughout the water column, with 3 genera (*Gyrodinium, Gymnodinium, Prorocentrum*) accounting for over 30% of the dinoflagellate community (Figure S2A). Vertical stratification was apparent among some of these ASVs. *Neoceratium* and *Gonyaulax* appeared to be restricted to the upper euphotic, while *Abedinium* had highest relative abundances at depths near the DCM. Other more abundant taxa such as *Prorocentrum* and *Gymnodinium* were distributed more or less evenly throughout the water column (Figure S2A). The majority of dinoflagellate ASVs lacked higher-level taxonomic classifications due to limited information in PR2 and SILVA 18S rRNA sequence databases.

ASVs attributed to ciliates and syndinians also consistently averaged more than 5% of the protistan community throughout the water column in all seasons (14% and 9%, respectively; Fig. 1; Supplemental Materials). The majority of the ciliate diversity fell within six phylogenetic groups of which spirotrichs were the most abundant (Figure S3). The other ciliate groups in order of relative abundances were oligohymenopheran, phyllopharyngean, litostome, colpodean and prostomastean ciliates. Among these latter groups, litostomes and oligohymenopherans had highest relative abundances below the euphotic zone. Similar to dinoflagellates, most syndinian ASVs were not classifiable with the PR2 database (v.12.1) or NCBI BLAST.

Radiolarian ASVs (1269 ASVs) were the only rhizarian clade present at more than 1% in any sample, and ranged from 4 to 14% of the community across all seasons (Fig. 1). Five subgroups accounted for the classifiable radiolarian assemblage, of which RAD-B accounted for the majority of sequence reads (331 K reads; Figure S3). Acantharian taxa were the second most abundant group within the radiolarian clade (286 K reads). Other less abundant taxa, in order of sequence abundance, included RAD-C (180 K reads), polycystines (80 K reads), and RAD-A (40 K reads).

Beyond SAR taxa, several other protistan groups were observed at low relative abundances with the exception of hacrobian taxa, which were comparable to ciliate abundances in the total community (30%; Fig. 1; Supplemental Materials). More than half of the hacrobian taxa were classified as haptophytes. Eight of twenty classifiable haptophyte taxa (out of 423 ASVs) were well represented, of which *Chrysochromulina* species were the most abundant (Fig. 1, S3). Choanoflagellates (opisthokonts) constituted a minor, but notable fraction of the total protistan community, with relative abundances greater than 5% occurring in the upper water column across all seasons (Fig. 1). Other opisthokonts (fungi, metazoa, 'other') were present at very minor relative abundances in part due to pre-filtration of the water samples which would have removed many of those taxa. Green algae (archaeplastids) occurred at low abundances in the community (generally <1% of total reads), but were present at >2% at or near the DCM with no clear seasonal variation (Fig. 1). ASVs of Amoebozoa and Excavata collectively accounted for less than 1% of the combined dataset, possibly as a consequence of known V4 amplicon primer bias (Gilbert et al., 2011).

3.3. The protistan community was vertically partitioned into three distinct communities

Non-metric multidimensional scaling (Bray-Curtis) including all 47 samples formed three well-defined clusters revealing that the protistan community structure from the surface (5 m) to 770 m was divided into three distinct zones according to depth: upper euphotic, lower euphotic and aphotic zones (Fig. 2A). Major transitions in community composition and richness occurred between the upper euphotic zone (5 m–75 m) and lower euphotic and shallow aphotic zone (100 m–175 m) and deep aphotic zone (300 m–700 m). The influence of depth on sample dissimilarity was most apparent within the aphotic cluster (300 m–770 m), with each depth forming somewhat distinct groups. The lower euphotic cluster was clearly distinguishable, but lacked strong seasonal or depth-related sub-groupings. Samples collected in the upper euphotic zone (5 m–75 m) encompassed sub-groupings that were related to sampling season (samples from April and August grouped separately from samples collected in the December samplings conducted one year apart). Hierarchical clustering analysis further supported that the majority of observed similarity between samples was on the basis of depth (Figure S4). The results of both statistical analyses were consistent with the separation between samples and clusters being the result of depth-dependent factors.

Measures of species richness and diversity (total number of ASVs and Simpson Index) were greatest for the 300 m–770 m aphotic cluster (1920 and 209 ASVs, respectively; Fig. 2B and C). Species richness was similar between the clusters associated with the upper euphotic zone (5 m–75 m) and the lower euphotic or shallow aphotic zone (1720 and 1740 ASVs, respectively; Fig. 2B). However, diversity based on the Simpson index was 3-fold greater in the upper euphotic zone relative to the lower euphotic or shallow aphotic zone (180 and 45.9, respectively;

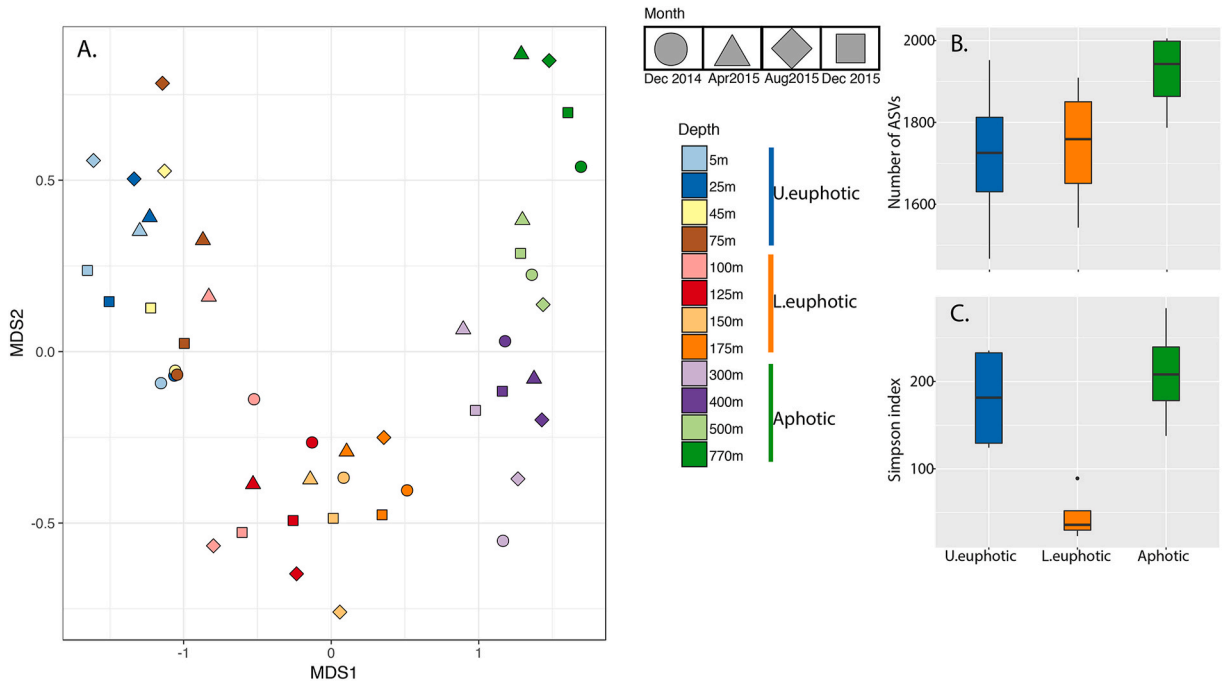

Fig. 2. Dissimilarity between samples using cDNA-based ASV relative abundances across depth and season. (A) NMDS plot (Bray-Curtis) of community compositions across all 47 samples: 12 depths, 3 seasons; Each point represents one sample. Vertical blue, orange and green bars represent zone cluster membership (Blue: Upper euphotic zone, Orange: Lower euphotic zone, Green: Aphotic zone); shapes represent the sampled months (Circle-Square: December, Triangle:April, Diamond: August). (B) Measures of ASV richness and diversity for each zone is illustrated using total number of ASV and (C) Simpson's diversity index calculated for each zone, respectively. Boxes illustrate the inter-quantile range (IQR) with the horizontal line indicating the median. Whiskers extend from the box to the furthest data within 1.5 × IQR.

Fig. 2C).

3.4. Protistan community composition of three well-defined, vertically distributed clusters

Our statistical analysis of sample dissimilarity suggested that differences in taxonomic composition across seasons and down the water column was largely attributable to depth. Estimates of diversity also implied that each cluster had differing levels of species richness and/or evenness (Fig. 2B and C). Accordingly, the spatial distribution of dominant taxa was investigated using ASVs averaged for the four seasonal samples at each depth. An UpSet plot color-coded for the three different zones revealed that a large number of ASVs were unique to each depth (Fig. 3; 12 columns on left side), but also that there was more similarity among communities (in terms of ASV richness and ASVs shared across depths (intersections)) within each of the depth zones (5 m–75 m, 100 m–175 m or 300 m–700 m), than between communities from different zones (Fig. 3). Intersections between different depth clusters were rare and occurred mostly on the borders of adjacent zones. There were no intersections between depths within the upper euphotic and aphotic zone, highlighting the difference in community structure between these two pelagic biomes.

Photosynthetic stramenopiles (diatoms, pelagophytes and other ochrophytes) were a significant fraction of the upper euphotic zone samples (13% total), and unclassified stramenopiles comprised an additional 7% (Fig. 4A). Diatoms and other ochrophytes were minor components in the lower euphotic zone (both at 1%), while pelagophytes were particularly abundant in the lower euphotic zone samples (18% of reads versus 2% in the upper euphotic zone; Fig. 4B). Haptophytes accounted for 7% and 9% of total reads in the upper euphotic and lower euphotic zones, respectively. Archaeplastids also accounted for 1% of reads within the lower euphotic zone samples (Fig. 4B).

Among known heterotrophic protistan groups, MAST ASVs were significant contributors to sun-lit depths, accounting for 17% of sequences in the upper euphotic zone and 11% in the lower euphotic zone (Fig. 4A and B; Supplemental Materials). Choanoflagellates were 6% of the community in the upper euphotic, substantially greater than this group's relative abundance in the lower euphotic and deep aphotic zones (≤1%; Fig. 4A and B). In contrast, radiolarian sequences in the upper euphotic and lower euphotic zone communities were approximately one third the relative abundances of this group in samples from the deep aphotic zone (5% and 4%, respectively; Fig. 4A and B). Dinoflagellate, ciliate and syndinian sequences were present at similar abundances in the two euphotic zones at approximately 21%, 10% and 7%, respectively. Relative abundances of ciliates and syndinians in the two euphotic zone clusters were approximately half their contributions in the deep aphotic zone, while the classifiable dinoflagellate contributions were little changed by depth (Fig. 4A and B versus 4C; Supplemental Materials).

Alveolate sequences comprised the greatest portion of the aphotic zone community composition (57% of sequenced reads; Fig. 4C versus 4 A,B). Dinoflagellates and ciliates accounted for more of this component of the community than any other single phylum (24% and 20%, respectively). Globally distributed parasitic alveolates within the order Syndiniales were 13% of the deep aphotic community. Radiolarians were the second most abundant taxa in the deep aphotic zone (14% of reads). These same samples were relatively devoid of classifiable photosynthetic stramenopiles (less than 1%), although heterotrophic stramenopiles (MAST) accounted for approximately 8% of the aphotic community (Fig. 4C). Haptophytes, which contain numerous mixotrophic species, accounted for 2% of the aphotic community. Unicellular opisthokonts (choanoflagellates) also constituted less than 1% of total reads in the samples from the deep aphotic zone, while metazoa were approximately 8% of reads.

3.5. Group-specific vertical distributions of dominant protists

Patterns of the vertical distributions observed in this study were

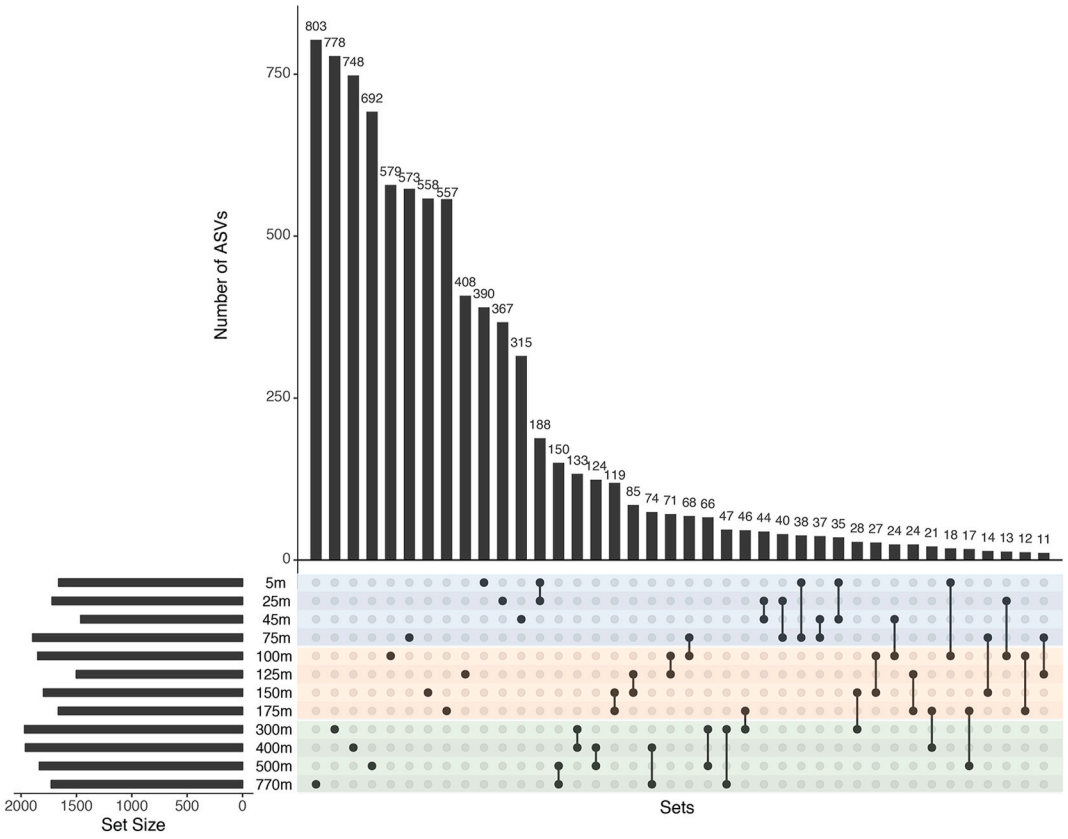

Fig. 3. UpSet plot illustrating shared ASVs (intersections) between depths averaged across the four seasons. Horizontal bars (Set Size) represent the number of ASVs within each depth, vertical bars represent the number of ASVs found within a sample set. Sets are the intersections between depths illustrated by shaded balls and sticks within the grid. Colored shading indicates the zone membership of the corresponding depths. i.e. blue, orange, green shading, correspond to upper euphotic, lower euphotic and aphotic zones, respectively.

unique for several of the dominant protistan groups, contributing to the observed depth-related differences in community structure. Diatoms were most abundant in the upper euphotic zone (5 m–75 m) at relatively unchanging abundances, followed by a steady decrease in abundances beginning at 75 m, to less than 2% of total reads below 100 m (Fig. 5A). Pelagophytes, on the other hand, were less abundant in the upper euphotic zone compared to their abundances in the lower euphotic zone (Fig. 5B). In particular, peak average abundances of pelagophytes (about 15% of sequence reads) occurred at 125 m and declined to <1% below 175 m. Haptophytes had the broadest distribution range, accounting for nearly 10% of the community from 45 m to 125 m, and averaged nearly 2% of the community below 300 m (Fig. 5C).

The heterotrophic taxa within the choanoflagellates and MAST groups were most abundant within the upper euphotic zone and decreased gradually with depth (Fig. 5D and E). Conversely, the heterotrophic taxa within the ciliate and radiolarian groups both increased gradually in relative abundances down the water column, and reached peak abundances at or near 770 m (Fig. 5F and G). The vertical distribution of ASVs classified as Syndiniales was strikingly similar to the ciliate and radiolarian distribution patterns (Fig. 5H), while dinoflagellates (Dinophyceae) increased gradually in relative abundances down the water column, but exhibited peak abundances near the base of the lower euphotic zone and shallow aphotic zone (175 m; Fig. 5I). The number of unclassifiable taxa also increased with depth (Fig. 5J). Unclassifiable sequences presumably included some metazoa, although the number of unclassifiable reads was ~1% of the total reads. Reanalysis of the entire dataset with or without the metazoan and unclassifiable reads yielded highly similar results.

3.6. ASV-specific vertical distributions among protists

As noted above, overall major group-specific distribution patterns were similar for radiolarians, ciliates and syndinians such that relative abundances generally increased with depth (Fig. 5G,F,H). In contrast, relative abundances of MAST were greatest in the upper euphotic zone and gradually decreased with depth (Fig. 5E), while haptophytes had subsurface maximal relative abundances between 45 m and 175 m (Fig. 5C). However, species-specific vertical distributions within each of these groups did not always conform to these general patterns (Fig. 6, S3).

Dominant syndinian ASVs, for example, containing taxa from dinogroups I, III, and IV, exhibited distinct vertical distributions. Among eleven abundant ASVs in the overall dataset, three had maximal relative abundances between 5 m and 175 m, with very few sequences of these ASVs observed below 175 m (ASVs 1–3; Fig. 6). Conversely, five ASVs had greater relative abundances at depth than in the upper water column (ASVs 5, 7, 9–11; Fig. 6) while two appeared to have maximal abundances at intermediate depths (ASVs 6, 8; Fig. 6). One ASV (ASV 4) had nearly constant abundances at all depths (Fig. 6).

Many of the ciliate taxa were present throughout the water column with little or no change in relative abundances (Figure S3). The vast majority of ciliate ASVs were identified as spirotrich ciliates. Spirotrichs displayed fairly constant abundances throughout the water column, along with phyllopharyngean and colpodean ciliates, both of which were present at much lower relative abundances than spirotrichs (Figure S3). However, ASVs attributable to oligohymenophoreans exhibited pronounced increases in relative abundance at depths ≥300 m, as did litostome ASVs to a lesser degree (Figure S3). These latter two ciliate groups were largely responsible for the overall trend of increasing

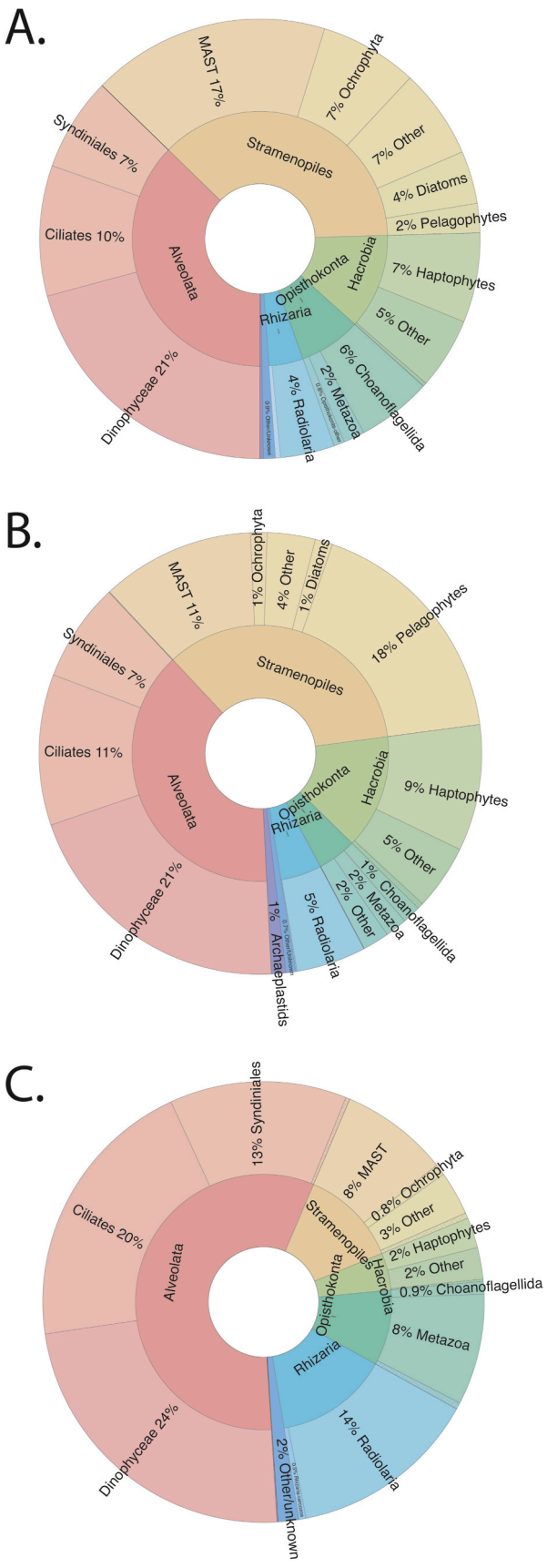

Fig. 4. Community composition of (A) upper euphotic, (B) lower euphotic, and (C) aphotic zones shown by krona plot.

ciliate sequence abundances in the deepest samples (Fig. 5F).

Some radiolarian ASVs also exhibited distinct vertical patterns. ASVs identified as acantharians, RAD-A, polycystines and other radiolarian taxa lacking higher classification (Rad.Other) had relative abundances that did not change appreciably with depth (Figure S3). However, RAD-B and RAD-C were marginally present in the upper euphotic zone and gradually increased to high relative abundances in the deepest samples. Relative abundances of acantharian taxa were 10-fold greater than all other radiolarian taxa combined at depths above 100 m.

The haptophyte assemblage had an overall vertical distribution with highest abundances between 45 m and 175 m (Fig. 5C) that was mirrored by the vertical distributions of most of the haptophyte ASVs observed in the study, although the depth of maximal abundances varied among the taxa from 45 m to 175 m (Figure S3). Similarly, the abundant MAST ASVs were most abundant in the upper euphotic zone and decreased with depth (Figure S3), as did the overall distribution of the MAST group (Fig. 5E).

4. Discussion

We characterized the vertical distribution and diversity of the protistan community across three seasons and twelve depths from 5 m to 770 m via sequencing of RNA transcripts (cDNA) of the V4 hypervariable region of the 18S rRNA gene in which more than 11,000 ASVs were recovered from 2.6 million rRNA reads across 47 samples. The most striking feature of our results was the marked changes in community structure across three depth ranges (5 m–75 m, 100 m–175 m and 300 m–700 m) driven by distribution patterns between, and in some cases within, major taxonomic groups. In contrast to the influence of depth on the overall protistan community structure, seasonal changes were not significant.

4.1. Three distinct protistan communities occupy the first 770 m of the water column at station ALOHA

Non-metric multidimensional scaling (NMDS) of Bray-Curtis dissimilarity between all 47 samples revealed that the protistan community from the upper euphotic to 770 m formed three distinct clusters according to depth (Fig. 2). In contrast, seasonality had a relatively small influence on community structure, albeit some groups such as diatoms did exhibit summer maxima (Fig. 1). Hierarchical clustering of all 47 samples also indicated statistically significant differences on the basis of depth (Figure S4). Moreover, large numbers of unique ASVs were observed at every depth sampled in this study (Fig. 3). Communities from depths below 175 m formed one cluster corresponding to the deep aphotic zone (300 m–770 m), whereas communities from near the ocean surface down to the shallow aphotic zone formed two well-defined clusters corresponding to the upper euphotic zone (5 m–45 m) and the lower euphotic to shallow aphotic zones (75 m–175 m; Fig. 2A). The latter cluster was co-located with the deep chlorophyll maximum, a permanent feature of this portion of the NPSG (Karl and Church, 2014; Figure S1).

A minor influence of seasonality on community structure was apparent only among samples collected in the upper euphotic zone (Fig. 2A). These findings are not surprising, as the greatest influence of seasonality would be anticipated near the ocean surface where seasonal ranges in temperature, light and other factors are greatest. Samples collected during August and April in the upper euphotic zone were separated (albeit marginally) from each other on the NMDS plot, and from samples collected during December. Samples collected on the two December dates clustered together (and away from August and April) despite the fact that the December sampling events were one year apart.

Seasonality was not apparent (i.e. their locations on the NMDS plot overlapped in Fig. 2A) among protistan communities collected from the lower euphotic zone (75 m–150 m). No clear groupings by season were observed in the lower euphotic despite reported seasonal changes in

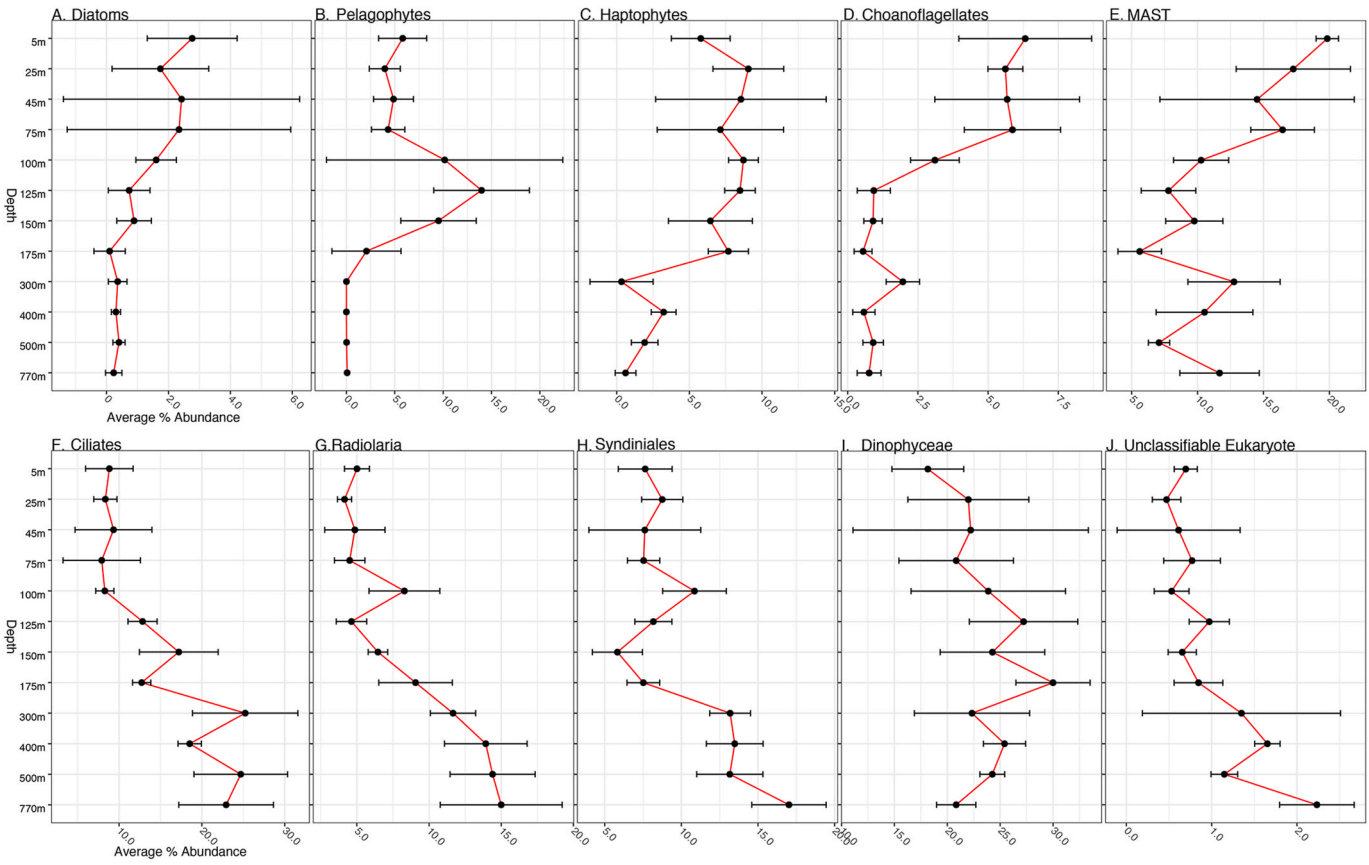

Fig. 5. Vertical distribution patterns of protistan groups that accounted for 5% or more of the total protistan community composition, and unclassified eukaryotic ASVs. Points indicate average percent abundance from samples taken in December 2014, April, August, and December 2015. Error bars illustrate the standard deviation between samples. The protistan groups represented are: (A) Diatoms, (B) Pelagophytes, (C) Haptophytes, (D) Choanoflagellates, (E) MAST, (F) Ciliates, (G) Radiolarians, (H) Syndinians, (I) Dinoflagellates and (J) Unclassified eukaryotes.

light energy and the position of the nutricline (Letelier et al., 2004; Fig. 2A). Differences in the relative influence of depth and season on protistan community composition between the upper euphotic and the lower euphotic were presumably a consequence of the strong gradients of light and nutrients, and wind-induced vertical mixing in the upper euphotic zone, establishing the "two-layered" euphotic zone typically observed in the NPSG (Coale and Bruland, 1987; Bryant et al., 2016).

In contrast to samples from the upper and lower euphotic zones, samples from the deep aphotic zone separated neatly by depth, not season (Fig. 2A). Communities from each sample collected at depths ≥300 m formed groupings unrelated to sampling season, which is not surprising, but it was unanticipated that samples from 300 m to 770 m would be distinct from one another. For example, all samples across seasons associated with 770 m grouped on the second axis, and did not overlap with other samples in the aphotic cluster (Fig. 2A). A similar grouping pattern was observed for samples collected from 300 m, 400 m and 500 m. The dissimilarity of communities observed at the various sampling depths ≥300 m implies considerable, depth-specific community complexity in the deep ocean. Interestingly, Boeuf et al. (2019) observed significant contributions of oligohymenophorean ciliates in sediment traps deployed at 4,000 m near station ALOHA, based on metatranscriptome analyses. High relative abundances of these ciliates were also observed in water samples collected at depths ≥300 m in the present study (Figure S3), and may indicate an important role for these heterotrophic protists in food web structure and organic matter processing in the deep ocean.

Estimates of total protistan species richness (total ASVs) observed in our study were greatest for the deep aphotic zone community (Fig. 2B), perhaps indicating the presence of endemic protistan species together with the presence of surface-dwelling protistan assemblages transported to the deep ocean. Species richness estimates between the upper and lower euphotic zones were somewhat comparable to each other, however both were substantially lower than species richness estimates in the deep aphotic zone. The Simpson diversity index, which takes into account the evenness of the community, was comparatively higher for the deep aphotic and the upper euphotic zones, while the index was much lower for the lower euphotic zone (Fig. 2C). We speculate that the strong dominance of the protistan community at and near the DCM by a relatively small number of phytoplankton species (e.g. pelagophytes) capable of exploiting this highly stable, selective ecosystem may explain the low diversity index observed for the protistan community in the lower euphotic zone (Fig. 4B).

Regardless of the specific causes of the vertical zonation of distinct protistan communities observed in our study, these findings have implications for food web structure, and presumably energy flow and elemental transformation in the water column at station ALOHA. Transitions in the vertical distribution of phytoplankton species in the euphotic zone might be expected due to strong gradients in light and nutrient availability, and will influence trophic structure as a consequence of differences in the size and composition of the dominant primary producers (Rii et al., 2016a, 2016b, 2018). More significantly, wholesale changes in community structure below the euphotic zone (Figs. 2A and 4), and depth-specific distributions of heterotrophic protist ASVs within some of the major protistan groups (Figs. 5 and 6, S3) indicate that the protistan taxa carrying out important ecological processes are largely distinct at various depths throughout the water column in this oceanic ecosystem.

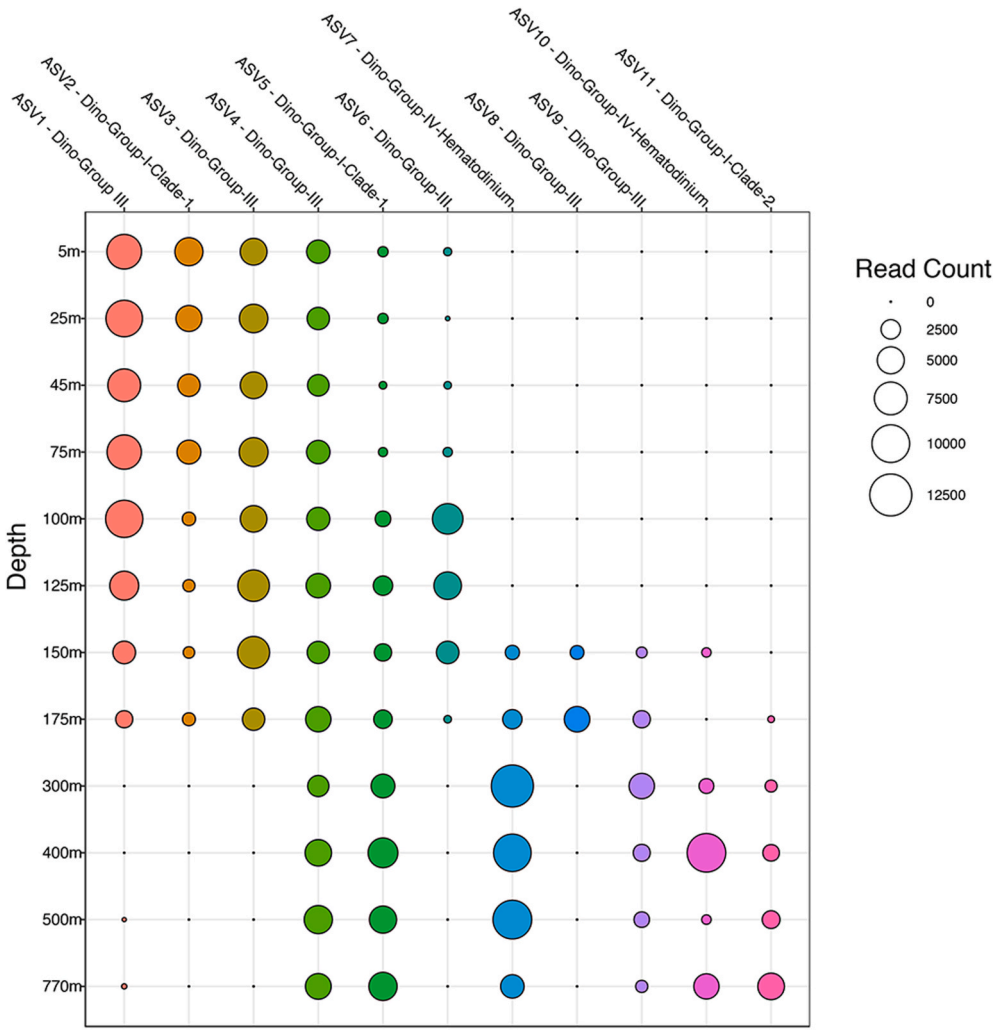

Fig. 6. Spatial distribution of the 11 most abundant syndinian ASVs. Balloon size is proportional to total read abundance. Some ASVS (1–3) are distributed throughout the entire euphotic zone or specific to the lower euphotic zone (6 & 8), while ASVs (7, 9–11) are preferential to the aphotic. ASVs 4 and 5 are shown distributed throughout the water column. Taxonomic information for each ASV is shown above each row.

4.2. Taxonomic and trophic diversity of the metabolically active protistan community at station ALOHA

We have shown that the metabolically active protistan community involved in ecosystem function and elemental cycling at station ALOHA are extremely diverse, and that the taxa exhibited specific vertical distributions at all levels of taxonomic resolution, from phylum to ASV. Phylogenetically distinct algae from three phyla (Dinoflagellate, Stramenopile, Haptophyte) having specific nutritional requirements and growth rates dominated the sun-lit depths (Figs. 1 and 4, S2, S3; Supplemental Material). An equally expansive pool of morphologically distinct heterotrophs with unique trophic strategies and metabolic capacities collectively colonized the entire water column from 5 m to 770 m (Figs. 1 and 4, S3; Supplemental Material). Putative parasites (ASVs classified within Syndiniales) were also prevalent throughout the water column. Interestingly, the dominant syndinian ASVs exhibited punctuated vertical distributions that differed from one another throughout the water column including those that appeared only in the euphotic, lower euphotic or aphotic zone (Fig. 6). The ubiquity with which diverse lineages of parasites are found in this study and throughout the global ocean (de Vargas et al., 2015; Pernice et al., 2016; Clarke et al., 2018) suggests that future ecosystem models should consider this potentially important but presently overlooked trophic behavior.

The expansive pool of taxonomic and trophic diversity found in this study has implications for improved ecosystem models in which bulk rates are used for photosynthetic and heterotrophic activity. Improving the resolution of ecosystem models in addition to the incorporation of less-appreciated trophic modes such as mixotrophy (Ward and Follows, 2016) and parasitism (Lafferty et al., 2006) may improve our understanding of ecosystem function and accuracy in predicting community level responses to environmental change.

Declaration of competing interest

The authors declare that they have no known competing financial interests or personal relationships that could have appeared to influence the work reported in this paper.

Acknowledgments

We are grateful to the SCOPE and HOT program staff (operations and science teams) for logistical support. Thanks also to Zhenfeng Liu and Michael D. Lee for advice and technical assistance in constructing a pipeline for the automated grouping of amplicon sequence variants and processing in R, and to Matthew Dean and Nathan Walworth for insightful conversations regarding the statistical analysis choices used in the multi-variate analysis of samples in this study. We acknowledge the captains and crew of the various research vessels that have supported

the HOT program, including the University of Hawai'i vessels RV 'Kilo Moana' and RV 'Ka'imikai-O- Kanaloa.' Funding: This work was supported by the Simons Foundation [Grants P49802 to DAC; #329108 and # 721223 to EFD], and the National Science Foundation [Grant 1737409 to DAC]. This work is a contribution of the Simons Collaboration on Ocean Processes and Ecology (SCOPE).

Appendix A. Supplementary data

Supplementary data to this article can be found online at https://doi.org/10.1016/j.dsr.2021.103494.

References

Berney, C., Ciuprina, A., Bender, S., Brodie, J., Edgcomb, V., Kim, E., Rajan, J., Parfrey, L. W., Adl, S., Audic, S., Bass, D., Caron, D.A., Cochrane, G., Czech, L., Dunthorn, M., Geisen, S., Glockner, F.O., Mahe, F., Quast, C., Kaye, J.Z., Simpson, A.G.B., Stamatakis, A., Del Campo, J., Yilmaz, P., de Vargas, C., 2017. UniEuk: time to speak a common language in protistology! J. Eukaryot. Microbiol. 64 (3), 407–411.

Blazewicz, S.J., Barnard, R.L., Daly, R.A., Firestone, M.K., 2013. Evaluating rRNA as an indicator of microbial activity in environmental communities: limitations and uses. ISME J. 7 (11), 2061–2068.

Boeuf, D., Edwards, B.R., Eppley, J.M., Hu, S.K., Poff, K.E., Romano, A.E., Caron, D.A., Karl, D.M., DeLong, E.F., 2019. Biological composition and microbial dynamics of sinking particulate organic matter at abyssal depths in the oligotrophic open ocean. Proc. Natl. Acad. Sci. U. S. A. 116 (24), 11824–11832.

Bolyen, E., Rideout, J.R., Dillon, M.R., Bokulich, N.A., Abnet, C.C., Al-Ghalith, G.A., Alexander, H., Alm, E.J., Arumugam, M., Asnicar, F., Bai, Y., Bisanz, J.E., Bittinger, K., Brejnrod, A., Brislawn, C.J., Brown, C.T., Callahan, B.J., Caraballo-Rodríguez, A.M., Chase, J., Cope, E.K., Da Silva, R., Diener, C., Dorrestein, P.C., Douglas, G.M., Durall, D.M., Duvallet, C., Edwardson, C.F., Ernst, M., Estaki, M., Fouquier, J., Gauglitz, J.M., Gibbons, S.M., Gibson, D.L., Gonzalez, A., Gorlick, K., Guo, J., Hillmann, B., Holmes, S., Holste, H., Huttenhower, C., Huttley, G.A., Janssen, S., Jarmusch, A.K., Jiang, L., Kaehler, B.D., Kang, K.B., Keefe, C.R., Keim, P., Kelley, S.T., Knights, D., Koester, I., Kosciolek, T., Kreps, J., Langille, M.G.I., Lee, J., Ley, R., Liu, Y.-X., Loftfield, E., Lozupone, C., Maher, M., Marotz, C., Martin, B.D., McDonald, D., McIver, L.J., Melnik, A.V., Metcalf, J.L., Morgan, S.C., Morton, J.T., Naimey, A.T., Navas-Molina, J.A., Nothias, L.F., Orchanian, S.B., Pearson, T., Peoples, S.L., Petras, D., Preuss, M.L., Pruesse, E., Rasmussen, L.B., Rivers, A., Robeson, M.S., Rosenthal, P., Segata, N., Shaffer, M., Shiffer, A., Sinha, R., Song, S.J., Spear, J.R., Swafford, A.D., Thompson, L.R., Torres, P.J., Trinh, P., Tripathi, A., Turnbaugh, P.J., Ul-Hasan, S., van der Hooft, J.J.J., Vargas, F., Vázquez-Baeza, Y., Vogtmann, E., von Hippel, M., Walters, W., Wan, Y., Wang, M., Warren, J., Weber, K. C., Williamson, C.H.D., Willis, A.D., Xu, Z.Z., Zaneveld, J.R., Zhang, Y., Zhu, Q., Knight, R., Caporaso, J.G., 2019. Reproducible, interactive, scalable and extensible microbiome data science using QIIME 2. Nat. Biotechnol. 10, 1038/s41587-019-0209-9.

Brum, J.R., Morris, J.J., Décima, M., Stukel, M.R., 2014. Mortality in the oceans: causes and consequences. In: Eco-DAS IX Symposium Proceedings. Chapter 2, vol. 16. Association for the Sciences of Limnology and Oceanography, pp. 16–48, 0.4319/ecodas.2014.978-0-9845591-3-8.

Bryant, J.A., Aylward, F.O., Eppley, J.M., Karl, D.M., Church, M.J., DeLong, E.F., 2016. Wind and sunlight shape microbial diversity in surface waters of the North Pacific Subtropical Gyre. ISME J. 10 (6), 1308–1322.

Calbet, A., Saiz, E., 2005. The ciliate-copepod link in marine ecosystems. Aquat. Microb. Ecol. 38, 157–167.

Callahan, B.J., McMurdie, P.J., Holmes, S.P., 2017. Exact sequence variants should replace operational taxonomic units in marker-gene data analysis. ISME J. 11 (12), 2639–2643.

Callahan, B.J., McMurdie, P.J., Rosen, M.J., Han, A.W., Johnson, A.J., Holmes, S.P., 2016. DADA2: high-resolution sample inference from Illumina amplicon data. Nat. Methods 13 (7), 581–583.

Canals, O., Obiol, A., Muhovic, I., Vaque, D., Massana, R., 2020. Ciliate diversity and distribution across horizontal and vertical scales in the open ocean. Mol Ecol 2020 1–16, 00.

Caron, D.A., 1994. Inorganic nutrients, bacteria, and the microbial loop. Microb. Ecol. 28 (2), 295–298.

Caron, D.A., Countway, P.D., Jones, A.C., Kim, D.Y., Schnetzer, A., 2012. Marine protistan diversity. Ann Rev Mar Sci 4, 467–493.

Caron, D.A., Hu, S.K., 2018. Are we overestimating protistan diversity in nature? Trends Microbiol. 27 (3), 197–205.

Clarke, L.J., Bestley, S., Bissett, A., Deagle, B.E., 2018. A globally distributed Syndiniales parasite dominates the Southern Ocean micro-eukaryote community near the sea-ice edge. ISME J. 13 (3), 734–737.

Coale, K.H., Bruland, K.W., 1987. Oceanic stratified euphotic zone as elucidated by 234Th: 238U disequilibria. Limnol. Oceanogr. 32 (1), 189–200.

Conway, J.R., Lex, A., Gehlenborg, N., 2017. UpSetR: an R package for the visualization of intersecting sets and their properties. Bioinformatics 33 (18), 2938–2940.

Countway, P.D., Gast, R.J., Dennett, M.R., Savai, P., Rose, J.M., Caron, D.A., 2007. Distinct protistan assemblages characterize the euphotic zone and deep sea (2500 m) of the western North Atlantic (Sargasso Sea and Gulf Stream). Environ. Microbiol. 9 (5), 1219–1232.

Coyne, K.J., Countway, P.D., Pilditch, C.A., Lee, C.K., Caron, D.A., Cary, S.C., 2013. Diversity and distributional patterns of ciliates in Guaymas Basin hydrothermal vent sediments. J. Eukaryot. Microbiol. 60 (5), 433–447.

de Vargas, C., Audic, S., Henry, N., Decelle, J., Mahe, F., Logares, R., Lara, E., Berney, C., Bescot, N., Probert, I., Carmichael, M., Poulain, J., Romac, S., Colin, S., Aury, J., Bittner, L., Chaffron, S., Dunthorn, M., Engelen, S., Flegontova, O., Guidi, L., Horak, A., Jaillon, O., Lima-Mendez, G., Lukes, J., Malviya, S., Morard, R., Mulot, M., Scalco, E., Siano, R., Vincent, F., Zingone, A., Dimier, C., Picheral, M., Searson, S., Kandels-Lewis, S., Coordinators, T.O., Acinas, S.G., Bork, P., Bowler, C., Gorsky, G., Grimsley, N., Hingamp, P., Iudicone, D., Not, F., Ogata, H., Pesant, S., Raes, J., Sieracki, M.E., Speich, S., Stemmann, L., Sunagawa, S., Weissenbach, J., Wincker, P., 2015. Eukaryotic plankton diversity in the sunlit ocean. E., K. Science 348 (6237), 1261601–1261605.

Edgcomb, V., Orsi, W., Taylor, G.T., Vdacny, P., Taylor, C., Suarez, P., Epstein, S., 2011. Accessing marine protists from the anoxic Cariaco Basin. ISME J. 5 (8), 1237–1241.

Edgcomb, V.P., 2016. Marine protist associations and environmental impacts across trophic levels in the twilight zone and below. Curr. Opin. Microbiol. 31, 169–175.

Edgcomb, V.P., Pachiadaki, M., 2014. Ciliates along oxyclines of permanently stratified marine water columns. J. Eukaryot. Microbiol. 61 (4), 434–445.

Field, C.B., Behrenfeld, M.J., James, T., Randerson, J.T., Falkowski, P.G., 1998. Primary production of the biosphere: integrating terrestrial and oceanic components. Science 281 (5374), 237–240.

Gilbert, J., Pawlowski, J., Christen, R., Lecroq, B., Bachar, D., Shahbazkia, H.R., Amaral-Zettler, L., Guillou, L., 2011. Eukaryotic richness in the abyss: insights from pyrotag sequencing. PloS One 6 (4), e18169.

Giner, C.R., Balague, V., Krabberod, A.K., Ferrera, I., Rene, A., Garces, E., Gasol, J.M., Logares, R., Massana, R., 2019. Quantifying long-term recurrence in planktonic microbial eukaryotes. Mol. Ecol. 28 (5), 923–935.

Giner, C.R., Forn, I., Romac, S., Logares, R., de Vargas, C., Massana, R., 2016. Environmental sequencing provides reasonable estimates of the relative abundance of specific picoeukaryotes. Appl. Environ. Microbiol. 82 (15), 4757–4766.

Giner, C.R., Pernice, M.C., Balague, V., Duarte, C.M., Gasol, J.M., Logares, R., Massana, R., 2020. Marked changes in diversity and relative activity of picoeukaryotes with depth in the world ocean. ISME J. 14 (2), 437–449.

Guillou, L., Bachar, D., Audic, S., Bass, D., Berney, C., Bittner, L., Boutte, C., Burgaud, G., de Vargas, C., Decelle, J., Del Campo, J., Dolan, J.R., Dunthorn, M., Edvardsen, B., Holzmann, M., Kooistra, W.H., Lara, E., Le Bescot, N., Logares, R., Mahe, F., Massana, R., Montresor, M., Morard, R., Not, F., Pawlowski, J., Probert, I., Sauvadet, A.L., Siano, R., Stoeck, T., Vaulot, D., Zimmermann, P., Christen, R., 2013. The Protist Ribosomal Reference database (PR2): a catalog of unicellular eukaryote small sub-unit rRNA sequences with curated taxonomy. Nucleic Acids Res. 41, D597–D604.

Guillou, L., Viprey, M., Chambouvet, A., Welsh, R.M., Kirkham, A.R., Massana, R., Scanlan, D.J., Worden, A.Z., 2008. Widespread occurrence and genetic diversity of marine parasitoids belonging to Syndiniales (Alveolata). Environ. Microbiol. 10 (12), 3349–3365.

Hartmann, M., Grob, C., Tarran, G.A., Martin, A.P., Burkill, P.H.S., Scanlan, D.J., Zubkov, M.V., 2012. Mixotrophic basis of Atlantic oligotrophic ecosystems. Proc. Natl. Acad. Sci. Unit. States Am. 109 (15), 5756–5760.

Hu, S.K., Campbell, V., Connell, P., Gellene, A.G., Liu, Z., Terrado, R., Caron, D.A., 2016a. Protistan diversity and activity inferred from RNA and DNA at a coastal ocean site in the eastern North Pacific. FEMS (Fed. Eur. Microbiol. Soc.) Microbiol. Ecol. 10, 1093/femsec/.

Hu, S.K., Campbell, V., Connell, P.E., Gellene, A.G., Liu, Z., Terrado, R., Caron, D.A., 2016b. Protistan diversity and activity inferred from RNA and DNA at a coastal ocean site in the eastern North Pacific. FEMS Microbiol. Ecol. 92 (4), fiw050.

Karl, D.M., Church, M.J., 2014. Microbial oceanography and the Hawaii Ocean Time-series programme. Nat. Rev. Microbiol. 12 (10), 699–713.

Karner, M.B., DeLong, E.F., Karl, D.M., 2001. Archael dominance in the mesopelagic zone of the Pacific Ocean. Nature 409, 507–510.

Konstantinidis, K.T., Braff, J., Karl, D.M., DeLong, E.F., 2009. Comparative metagenomic analysis of a microbial community residing at a depth of 4,000 meters at station ALOHA in the North Pacific subtropical gyre. Appl. Environ. Microbiol. 75 (16), 5345–5355.

Lafferty, K.D., Dobson, A.P., Kuris, A.M., 2006. Parasites dominate food web links. Proc. Natl. Acad. Sci. U. S. A. 103 (30), 11211–11216.

Letelier, R.M., Karl, D.M., Abbot, M.R.B., Bidigare, R.R., 2004. Light driven seasonal patterns of chlorophyll and nitrate in the lower euphotic zone of the North Pacific Subtropical Gyre. Limnol. Oceanogr. 49 (2), 508–519.

Lima-Mendez, G., Faust, K., Henry, N., Decelle, J., Colin, S., Carcillo, F., Chaffron, J.S., Ignacio-Espinosa, C., Roux, S., Vincent, F., Bittner, L., Darzi, Y., Wang, J., Audic, S., Berline, L., Bontempi, G., Cabello, A.M.C., Cornejo-Castillo, F.M., d'Ovidio, F., Meester, L.D., Ferrera, I., Garnet-Delmas, M., Guidi, L., Lara, E., Pesant, S., Royo-Llonch, M., Salazar, G., Sanchez, P., Sebastian, M., Souffreau, C., Dimier, C., Picheral, M., Searson, S., Kandels-Lewis, S., Gorsky, G., Not, F., Ogata, H., Speich, S., Stemmann, L., Weissenbach, J., Wincker, P., Acinas, S.G., Suanagawa, S., Bork, P., Sullivan, M.B., Karsenti, E., Bowler, C., de Vargas, C., Raes, J., 2015. Determinants of community structure in the global plankton interactome. L. Science 348 (6237).

Malmstrom, R.R., Coe, A., Kettler, G.C., Martiny, A.C., Frias-Lopez, J., Zinser, E.R., Chisholm, S.W., 2010. Temporal dynamics of prochlorococcus ecotypes in the atlantic and pacific oceans. ISME J. 4 (10), 1252–1264.

Mars Brisbin, M., Conover, A.E., Mitarai, S., 2020. Influence of regional oceanography and hydrothermal activity on protist diversity and community structure in the okinawa trough. Microb. Ecol. 80 (4), 746–761.

Mende, D.R., Bryant, J.A., Aylward, F.O., Eppley, J.M., Nielsen, T., Karl, D.M., DeLong, E.F., 2017. Environmental drivers of a microbial genomic transition zone in the ocean's interior. Nat Microbiol 2, 1367–1373.
Obiol, A., Giner, C.R., Sanchez, P., Duarte, C.M., Acinas, S.G., Massana, R., 2020. A metagenomic assessment of microbial eukaryotic diversity in the global ocean. Mol Ecol Resour 20 (3), 718–731.
Orsi, W., Edgcomb, V., Jeon, S., Leslin, C., Bunge, J., Taylor, G.T., Varela, R., Epstein, S., 2011. Protistan microbial observatory in the cariaco basin, caribbean. II. Habitat specialization. ISME J. 5 (8), 1357–1373.
Pasulka, A., Hu, S.K., Countway, P.D., Coyne, K.J., Cary, S.C., Heidelberg, K.B., Caron, D. A., 2019. SSU-rRNA gene sequencing survey of benthic microbial eukaryotes from guaymas basin hydrothermal vent. J. Eukaryot. Microbiol. 66, 637–653.
Pasulka, A.L., Landry, M.R., Taniguchi, D.A.A., Taylor, A.G., Church, M.J., 2013. Temporal dynamics of phytoplankton and heterotrophic protists at station ALOHA. Deep Sea Res. Part II Top. Stud. Oceanogr. 93, 44–57.
Pernice, M.C., Forn, I., Gomes, A., Lara, E., Alonso-Saez, L., Arrieta, J.M., del Carmen Garcia, F., Hernando-Morales, V., MacKenzie, R., Mestre, M., Sintes, E., Teira, E., Valencia, J., Varela, M.M., Vaque, D., Duarte, C.M., Gasol, J.M., Massana, R., 2015. Global abundance of planktonic heterotrophic protists in the deep ocean. ISME J. 9 (3), 782–792.
Pernice, M.C., Giner, C.R., Logares, R., Perera-Bel, J., Acinas, S.G., Duarte, C.M., Gasol, J. M., Massana, R., 2016. Large variability of bathypelagic microbial eukaryotic communities across the world's oceans. ISME J. 10 (4), 945–958.
Poulin, R., 2010. Network analysis shining light on parasite ecology and diversity. Trends Parasitol. 26 (10), 492–498.
Pruesse, E., Quast, C., Knittel, K., Fuchs, B.M., Ludwig, W., Peplies, J., Glockner, F.O., 2007. SILVA: a comprehensive online resource for quality checked and aligned ribosomal RNA sequence data compatible with ARB. Nucleic Acids Res. 35 (21), 7188–7196.
R_Core_Team, 2020. R: A Language and Environment for Statistical Computing. R Foundation for Statistical Computing, Vienna, Austria.
Rii, Y.M., Bidigare, R.R., Church, M.J., 2018. Differential responses of eukaryotic phytoplankton to nitrogenous nutrients in the North pacific subtropical gyre. Frontiers in Marine Science 5 (92), 1–17.
Rii, Y.M., Duhamel, S., Bidigare, R.R., Karl, D.M., Repeta, D.J., Church, M.J., 2016a. Diversity and productivity of photosynthetic picoeukaryotes in biogeochemically distinct regions of the South East Pacific Ocean. Limnol. Oceanogr. 61 (3), 806–824.
Rii, Y.M., Karl, D.M., Church, M.J., 2016b. Temporal and vertical variability in picophytoplankton primary productivity in the North Pacific Subtropical Gyre. Mar. Ecol. Prog. Ser. 562, 1–18.
Scharek, R., Tupas, L.M., Karl, D.M., 1999. Diatom fluxes to the deep sea in the oligotrophic North Pacific gyre at Station ALOHA. Mar. Ecol. Prog. Ser. 182, 55–67.
Sherr, E.B., Sherr, B.F., 2002. Significance of predation by protists in aquatic microbial food webs. Antonie Leeuwenhoek 81, 293–308.
Stoeck, T., Bass, D., Nebel, M., Christen, R., Jones, M.D., Breiner, H.W., Richards, T.A., 2010. Multiple marker parallel tag environmental DNA sequencing reveals a highly complex eukaryotic community in marine anoxic water. Mol. Ecol. 19 (1), 21–31.
Stoeck, T., Behnke, A., Christen, R., Amaral-Zettler, L., Rodriguez-Mora, M.J., Chistoserdov, A., Orsi, W., Edgcomb, V.P., 2009. Massively parallel tag sequencing reveals the complexity of anaerobic marine protistan communities. BMC Biol. 7 (72).
Unrein, F., Gasol, J.M., Not, F., Forn, I., Massana, R., 2014. Mixotrophic haptophytes are key bacterial grazers in oligotrophic coastal waters. ISME J. 8 (1), 164–176.
Ward, B.A., Dutkiewicz, S., Jahn, O., Follows, M.J., 2012. A size-structured food-web model for the global ocean. Limnol. Oceanogr. 57 (6), 1877–1891.
Ward, B.A., Follows, M.J., 2016. Marine mixotrophy increases trophic transfer efficiency, mean organism size, and vertical carbon flux. Proc. Natl. Acad. Sci. U. S. A. 113 (11), 2958–2963.
Weiss, S., Xu, Z.Z., Peddada, S., Amir, A., Bittinger, K., Gonzalez, A., Lozupone, C., Zaneveld, J.R., Vázquez-Baeza, Y., Birmingham, A., Hyde, E.R., Knight, R., 2017. Normalization and microbial differential abundance strategies depend upon data characteristics. Microbiome 5 (27).
Worden, A.Z., Follows, M.J., Giovannoni, S.J., Wilken, S., Zimmerman, A.E., Keeling, P. J., 2015. Environmental science. Rethinking the marine carbon cycle: factoring in the multifarious lifestyles of microbes. Science 347 (6223), 1257594.
Xu, D., Li, R., Hu, C., Sun, P., Jiao, N., Warren, A., 2017. Microbial eukaryote diversity and activity in the water column of the south China sea based on DNA and RNA high throughput sequencing. Front. Microbiol. 8 (1121).